Metabonomic Analysis Reveals Efficient Ameliorating Effects of Acupoint Stimulations on the Menopause-caused Alterations in Mammalian Metabolism

Limin Zhang[1], Yulan Wang[1,5], Yunxiang Xu[3], Hehua Lei[1], Ying Zhao[1], Huihui Li[1], Xiaosheng Lin[2], Guizhen Chen[2] & Huiru Tang[1,4]

[1]CAS Key Laboratory of Magnetic Resonance in Biological Systems, State Key Laboratory of Magnetic Resonance and Atomic and Molecular Physics, Wuhan Centre for Magnetic Resonance, Biospectroscopy and Metabomics Centre, Wuhan Institute of Physics and Mathematics, Chinese Academy of Sciences, Wuhan 430071, China, [2]Affiliated BaoAn TCM Hospital, Guangzhou University of Chinese Medicine, Shenzhen, 518101, China, [3]Clinical Medical College of Acupuncture and Rehabilitation, Guangzhou University of Chinese Medicine, Guangzhou, 510405, P. R. China, [4]State Key Laboratory of Genetic Engineering, Biospectroscopy and Metabolomics, School of Life Sciences, Fudan University, Shanghai 200433, P. R. China, [5]Collaborative Innovation Center for Diagnosis and Treatment of Infectious Diseases, Zhejiang University, 866 Yuhangtang Road, Hangzhou 310058, P. R. China.

Acupoint stimulations are effective in ameliorating symptoms of menopause which is an unavoidable ageing consequence for women. To understand the mechanistic aspects of such treatments, we systematically analyzed the effects of acupoint laser-irradiation and catgut-embedding on the ovariectomy-induced rat metabolic changes using NMR and GC-FID/MS methods. Results showed that ovariectomization (OVX) caused comprehensive metabolic changes in lipid peroxidation, glycolysis, TCA cycle, choline and amino acid metabolisms. Both acupoint laser-irradiation and catgut-embedding ameliorated the OVX-caused metabonomic changes more effectively than hormone replacement therapy (HRT) with nilestriol. Such effects of acupoint stimulations were highlighted in alleviating lipid peroxidation, restoring glucose homeostasis and partial reversion of the OVX-altered amino acid metabolism. These findings provided new insights into the menopause effects on mammalian biochemistry and beneficial effects of acupoint stimulations in comparison with HRT, demonstrating metabonomics as a powerful approach for potential applications in disease prognosis and developments of effective therapies.

Menopause is defined as the permanent cessation of menstruation resulting from diminished ovarian production of female hormones including estrogen and progesterone[1]. Whilst natural menopause occurs in women as part of the aging process, ovariectomy also causes so-called surgical menopause or induced-menopause. However, both natural and surgical menopauses always lead to deficiency of the circulating estrogens[2] accompanied with oxidative stresses to a number of organs especially liver and kidney[3]. Such deficiency also results in dysfunctions of hypothalamic-pituitary-ovarian axis and adrenal glands[4]. Therefore, climacteric women often experience more than one physical and psychological symptoms or complaints including hot flashes[5], loss of bone mass[6], mood changes and even depression. More serious menopausal effects include osteoporosis and/or some chronic diseases including cardiovascular diseases[7], Alzheimer's disease and colorectal cancer[8], which seriously compromises the life quality of patients.

In clinical settings, hormone replacement therapy (HRT) is the treatment of first choice to alleviate menopausal symptoms and to protect women from some resultant chronic diseases such as cardiovascular disease. This is because that estrogens can regulate serum lipids[9] and produce other vasoactive molecules such as nitric oxide[10] and prostaglandins[11]. However, HRT has many well-known side-effects including cholelethiasis, thromboembolism and especially increased risks for both breast and ovarian cancer[8]. Epidemiological studies showed that each year of using HRT increased the breast cancer risk[12] by a factor of 1.023. Compared with those who never had HRT, women under HRT showed the incidence increase of 1.38 (95% confidence interval) and 1.44 (95% confidence interval) for all ovarian cancers and epithelial ovarian cancer respectively[13].

Table 1 | Data for plasma clinical biochemistry and fatty-acids composition from rats treated with sham operation, OVX (A), OVX followed with nilestriol supplementation (B), acupoint laser-irradiation (C) and catgut embedding (D)

	Sham	A	B	C	D
ALT (IU/L)	25.20 ± 3.96	34.40 ± 4.25 (0.000)ᵃ,ᵇ	35.50 ± 7.59 (0.000)	25.40 ± 3.72 (0.893)	25.56 ± 7.23 (0.890)
AST (IU/L)	98.20 ± 17.11	156.60 ± 7.14 (0.000)	146.92 ± 10.93 (0.000)	95.53 ± 11.49 (0.755)	101.78 ± 17.80 (0.740)
Glc (mmol/L)	7.95 ± 0.34	5.60 ± 0.71 (0.014)	6.27 ± 0.53 (0.028)	7.17 ± 0.77 (1.000)	7.51 ± 0.77 (0.317)
TG (mmol/L)	1.30 ± 0.52	0.58 ± 0.14 (0.002)	0.83 ± 0.20 (0.033)	0.95 ± 0.13 (0.127)	0.93 ± 0.13 (0.275)
HDL (mmol/L)	0.67 ± 0.25	0.83 ± 0.15 (0.041)	0.89 ± 0.14 (0.023)	0.70 ± 0.09 (0.707)	0.71 ± 0.07 (0.599)
LDL (mmol/L)	0.16 ± 0.04	0.13 ± 0.02 (0.015)	0.15 ± 0.03 (0.124)	0.16 ± 0.04 (0.814)	0.16 ± 0.03 (0.825)
Urea (μmol/L)	5.53 ± 1.08	7.26 ± 1.03 (0.001)	7.06 ± 1.18 (0.006)	4.78 ± 0.80 (0.073)	5.76 ± 1.34 (0.673)
CHOL(mmol/L)	2.08 ± 0.28	2.94 ± 0.43 (0.001)	2.77 ± 0.68 (0.000)	2.44 ± 0.37 (0.001)	2.37 ± 0.25 (0.003)
AKP (IU/L)	119.5 ± 19.38	128.70 ± 10.74 (0.203)	78.30 ± 10.59 (0.000)	133.50 ± 9.75 (0.843)	128.00 ± 16.48 (0.314)
TP (g/L)	66.06 ± 8.34	71.61 ± 8.41 (0.146)	76.59 ± 7.34 (0.006)	72.98 ± 5.09 (0.025)	61.14 ± 3.17 (0.094)
ALB (g/L)	39.93 ± 3.79	42.03 ± 4.46 (0.373)	46.16 ± 4.25 (0.003)	42.96 ± 4.17 (0.134)	35.87 ± 2.74 (0.084)
TBL (μmol/L)	4.69 ± 2.26	5.71 ± 1.04 (0.051)	6.43 ± 1.22 (0.041)	5.98 ± 0.83 (0.124)	6.07 ± 0.98 (0.972)
DBL (μmol/L)	0.81 ± 0.31	0.56 ± 0.30 (0.121)	0.47 ± 0.11 (0.008)	0.60 ± 0.21 (0.511)	0.78 ± 0.33 (1.000)
C18:0 (mg/L)ᶜ	2650.39 ± 791.28	1846.93 ± 416.25 (0.036)	3181.16 ± 457.30 (0.021)	2222.28 ± 477.19 (0.047)	2446.37 ± 335.78 (0.231)
C20:3n6 (mg/L)ᶜ	54.56 ± 19.44	66.34 ± 22.49 (0.002)	86.19 ± 31.04 (0.000)	74.53 ± 9.56 (0.000)	51.92 ± 17.77 (0.516)
C20:4n6 (mg/L)ᶜ	480.84 ± 142.69	1010.75 ± 338.19 (0.003)	1159.35 ± 168.22 (0.000)	666.05 ± 138.09 (0.059)	854.00 ± 243.96 (0.056)
C20:5n3 (mg/L)ᶜ	44.25 ± 10.14	66.63 ± 24.18 (0.043)	85.63 ± 28.33 (0.028)	65.53 ± 15.80 (0.013)	36.32 ± 11.24 (0.091)
C22:5n3 (mg/L)ᶜ	39.18 ± 12.14	69.62 ± 19.95 (0.006)	82.80 ± 9.33 (0.000)	69.10 ± 24.11 (0.013)	52.53 ± 12.41 (0.087)
C22:6n3 (mg/L)ᶜ	334.03 ± 110.90	565.62 ± 185.83 (0.017)	729.06 ± 73.03 (0.000)	475.69 ± 139.87 (0.070)	425.81 ± 102.48 (0.093)

ᵃp-values in parenthesis were obtained from the Student's tests against the sham group.
ᵇRed colored numbers denote a significant increase whereas the blue colored ones indicate a significant decrease and the black colored ones denote no significant changes in the treated rats (A, B, C, and D) compared to the sham group.
ᶜFatty acids were measured using GC-FID/MS.

Phytoestrogens such as coumestans, prenylated flavonoids and isoflavones are suggested to be alternatives to HRT. These natural products showed some therapeutic effects probably due to their bindings to estrogen receptors (ER) with higher affinity for ER-β than ER-α[14]. However, many important aspects of their effective utilizations in clinical settings remain to be fully elucidated including their absorptive bioavailability and pharmacokinetics, *in vivo* metabolisms, distributions and side-effects.

Acupuncture is reported as another alternative therapy to HRT which is normally conducted by stimulating certain points known as acupoints with fine needles or electrical pulses[15,16]. More recently, some other acupoint stimulation techniques have also been developed such as acupoint laser-irradiation[17] and catgut-embedding[18]. In clinical trials, electrical acupuncture has shown effectiveness in reducing menopausal symptoms such as hot flashes and vasomotor symptoms for 45 women aged 48–63 years-old[15,16]. Such efficacy probably results from the effects of acupoint stimulation on the physiological regulations in human body[19]. For example, acupoint stimulation may stimulate releases of hormones and neurotransmitters in the central nervous system which in turn assists the regulation of human physiological processes so as to promote physical and emotional well-being[20]. Stimulation to the acupoint *Shenshu* (BL 23) (Fig. S1) with laser-irradiation has shown some therapeutic effects on overiectomized rats[17]. Therefore, many international regulatory bodies have endorsed the use of acupuncture for certain conditions including the National Institutes of Health in United States[21], the National Health Service of the United Kingdom[22], the World Health Organization[23], and the National Center for Complementary and Alternative Medicine[24].

However, the mechanistic aspects of acupuncture remain vague and need investigating even though large bodies of information and experience have been accumulated with animal models and in clinical practice. Since menopausal processes involve a number of hormones, metabolic changes are expected to be associated with the menopause development and thus effective interventions. Metabolic response to acupuncture (or acupoint stimulations) ought to be closely associated with the effectiveness and molecular mechanism of acupuncture treatments. Therefore, measuring metabolite compositional changes is a potentially important approach.

Metabonomics has been proven to be suitable for obtaining the metabolic information associated with progression of many diseases. Metabonomic analysis is featured with the combination of metabolite detection using spectroscopic techniques, such as nuclear magnetic resonance (NMR) and mass spectrometry (MS), and multivariate data analysis. Such approaches offered a holistic overview of integrated metabolic response of an organism to stimuli[25,26]. As a systems biology approach, metabonomic analysis has revealed metabolic characteristics associated with a number of diseases, such as parasitic diseases[27,28], cancers[29], obesity[30,31], diabetes[32,33] and inflammatory bowel diseases[34,35]. To the best of our knowledge, metabonomics strategies have not been employed for systematically investigating the characteristics of postmenopausal syndromes and therapeutic effects for the time being.

In this study, we analyzed the ovariectomy-induced metabonomic changes in rats and the therapeutic effects of acupoint stimulations with laser-irradiation and catgut-embedding in comparison with HRT by using the combined NMR and GC-FID/MS technologies. Our results showed that ovariectomy induced marked metabolic changes and acupoint stimulations had better therapeutic effects than traditional HRT in terms of the metabolic restoration to normality. This demonstrated that metabonomic approach could play pivotal roles for understanding the mechanistic aspects of effective therapies.

Results

Clinical chemistry results (Table 1) indicated that ovariectomy (OVX) caused significant elevations of ALT, AST, TBL, urea, t-CHOL and HDL together with level decreases for glucose, TG and LDL in rat serum compared with both the sham and normal groups. Treatments with nilestriol supplement, acupoint catgut-embedding and laser-irradiation reversed these changes to various degrees. Such is highlighted by significant depletion of ALT, AST, urea, t-CHOL and HDL accompanied with elevation of glucose, triglycerides and LDL compared with the OVX rats. However, nilestriol-treated group did not completely reverse the OVX-induced changes with the levels of ALT, AST and HDL remaining significantly higher whilst the levels for glucose and triglycerides remaining significantly lower than the sham group (Table 1). In fact, nilestriol treatment significantly elevated the levels of ALT, HDL, TP and ALB even further compared with OVX. In

contrast, both catgut-embedding and laser-irradiation stimulations completely restored the OVX-caused all changes to normality (compared with the sham group) with only exception for total cholesterol level (Table 1).

^{1}H NMR spectra were recorded for plasma samples (Fig. S2) from the sham and ovariectomized rats as well as the OVX rats treated with nilestriol, catgut-embedding and laser-irradiation acupoint-stimulations, respectively. The resonances were assigned to metabolites (Supplementary Table 1) based on the literature data[36,37] and further confirmed individually by a series of two-dimensional NMR experiments. These spectra contained signals mainly from lipoprotein-containing fatty acids, glycoproteins, glucose, amino acids, carboxylic acids such as lactate and 3-hydroxybutyrate (3-HB), and choline metabolites. Visual inspection revealed that OVX induced clear decrease in the level of glucose (δ 5.23) accompanied with elevation of 3-HB. Such changes were reversed to various extents by treatments with nilestriol, catgut-embedding and laser-irradiation acupoint-stimulations. More detailed metabolite changes and their significance are obtainable using multivariate data analysis.

The scores plot from principal component analysis (PCA) shows inter-group metabolic differences, where each point represents a rat plasma metabonome and the distance between data-points reflects the scale of their metabolic differences. Our results indicated that OVX induced marked metabolic changes in rat plasma (Fig. 1) whereas treatments with nilestriol supplement, acupoint catgut-embedding and laser-irradiation reversed such changes to various degrees. It is also obvious that acupoint stimulations had better ameliorative effects than HRT with nilestriol (Fig. 1). No differences were observed in the plasma metabonomes between control and sham groups (Fig. S3), indicating complete recovery for any changes resulting from the sham operation at the time point of examination.

Pair-wise comparative OPLS-DA was further conducted to uncover detailed metabolic changes induced by ovariectomy and the aforementioned treatments (Fig. S4 and Table S2). Compared with sham group, OVX caused significant elevations of unsaturated fatty acids, a number of amino acids, choline metabolites (choline, PC and GPC), ketone bodies (3-HB and acetoacetate), glycoproteins (NAG and OAG), acetate and creatine (Fig. 2a). OVX operation also resulted in significant reductions in the levels of triglycerides and glucose in rat plasma (Fig. 2a).

Nilestriol treatment (HRT) reversed some of the OVX-induced changes especially for lysine, arginine, glycine, citrate, creatine, acetate, NAG and OAG. However, the rest OVX-induced metabolic changes remained (Fig. 2a). In contrast, acupoint stimulations with laser-irradiation and catgut embedding reversed the OVX-induced metabolic changes more comprehensively than HRT (Fig. 2a). Upon such acupoint interventions, many metabolites returned to their normal levels for sham rats including glucose, ketone bodies, creatine, acetate, citrate, glycine and NAG. Acupoint laser-irradiation further reversed the changes in leucine, isoleucine and valine (Fig. 2a) whilst catgut-embedding also completely reversed the OVX-induced changes in lysine, arginine, tyrosine and phenylalanine (Fig. 2a). Semi-quantitative analysis of the metabolite levels against those of the sham rats illustrated that acupoint stimulations with both laser-irradiation and catgut-embedding had much better ameliorative effects than HRT in terms of reversing the OVX-induced metabolic changes (Fig. 2b). However, neither treatment restored the OVX-induced changes in OAG, unsaturated fatty acids (UFA), polyunsaturated fatty acids (PUFA) and choline metabolites (Fig. 2). Results obtained from the diffusion-edited NMR spectra[36,38] confirmed such observations for both UFA and PUFA (Fig. S5).

Furthermore, fatty acid compositional analysis revealed that OVX led to significant level decreases for C18:0 and elevation of polyunsaturated fatty acids including C20:3n6, C20:4n6, C20:5n3, C22:5n3 and C22:6n3 (Table 1 and Fig. 2b). Three treatments had fairly different therapeutic effects on the OVX-induced changes in fatty acids. HRT failed to reverse any of the OVX-induced fatty acid changes to normality (i.e., the levels in sham group). On one hand, HRT overly reversed the changes of C18:0 whilst inadequately restored the changes of C20:5n3. On the other hand, HRT caused even further increases in the levels of C20:4n6, C20:3n6, C22:5n3 and C22:6n3 (Table 1 and Fig. 2b) from OVX operation compared with sham group. In contrast, acupoint laser-irradiation completely restored the OVX-induced C20:4n6 elevation to normality and partially reversed the OVX-caused changes for C18:0, C20:5n3, C22:5n3 and C22:6n3. More strikingly, acupoint stimulation with catgut-embedding completely restored the OVX-induced changes to normality (i.e., the sham group levels) for all fatty acids (Table 1 and Fig. 2b).

Discussion

The ovariectomized (OVX) rats are widely accepted menopausal models to represent the most important clinical features of estrogen deficiency in the adult human. Hormone replacement therapy (HRT) is the commonly employed clinical treatments. Clinical investigations showed that acupoint stimulations such as acupuncture treatments significantly reduced the number of hot flashes associated with menopause[16] although the mechanistic aspects remained debatable[39] with limited biochemistry evidences. In theory, OVX-caused menopause induces metabolic changes and the effectiveness of a therapeutic intervention ought to be reflected in the extents of reversing such changes.

Here, we systematically analyzed the OVX-caused metabolic alterations and possible therapeutic effects of acupoint stimulations (laser-irradiation and catgut-embedding) and HRT in terms of metabolic restoration upon treatments. We found that OVX caused systematic changes in multiple metabolic pathways (Fig. 3) which were reversed to various extents when treated with acupoint stimulations and HRT. Acupoint stimulations including both laser-irradiation and catgut-embedding were much more effective in reversing the OVX-induced metabolic changes than classical HRT; catgut-embedding was more effective than laser-irradiation. To the best of our knowledge, this is the first time to discover that acupoint stimulations can rebalance the metabolic disruptions caused by OVX-induced estrogen deficiency.

First, this study revealed that OVX-induced estrogen deficiency caused prominent changes in lipid metabolism with a significant elevation in the PUFA levels (Fig. 2) and depletion of saturated fatty acids and triglycerides (Table 1). We also observed concurrent elevation of lipid β-oxidation products (3-HB and acetoacetate) in the plasma of OVX rats (Fig. 2). The existing literature works appeared to have two contradictory notions for the effects of estrogen-deficiency on lipid metabolism. On one hand, the expression of peroxisome proliferators-activated receptor-α (PPAR-α) was decreased in the OVX rat liver accompanied with increased expressions of sterol regulatory element-binding proteins (SREBPs)[40]. This implied that the down-regulation of lipid oxidation and up-regulation of lipogenesis were associated with menopause resulting in fatty liver observed for both the OVX rats and postmenopausal women[40]. On the other hand, enhancement of lipid peroxidation in liver and kidney of the OVX rats was reported[3] contributing to the high atherosclerosis prevalence in postmenopausal women[10]. Our results seemingly supported both of these contradictory observations. The elevation of ketone bodies indicated OVX-induced enhancement for fatty-acid oxidation in peroxisomes whereas the level rises for PUFAs indicated a decreased lipid oxidation with concurrent increases in the biosynthesis of PUFAs via desaturation. However, these findings imply that OVX concurrently causes up-regulation of peroxisomal β-oxidaton but down-regulation of mitochondrial β-oxidaton. This is supported by the decreased gene expression of carnitine palmitoyltransferase I (CPT1) for OVX rats[41] since mitochondrial β-oxidaton requires carnitine acyltransferase I and II as transporters whereas peroxisomal
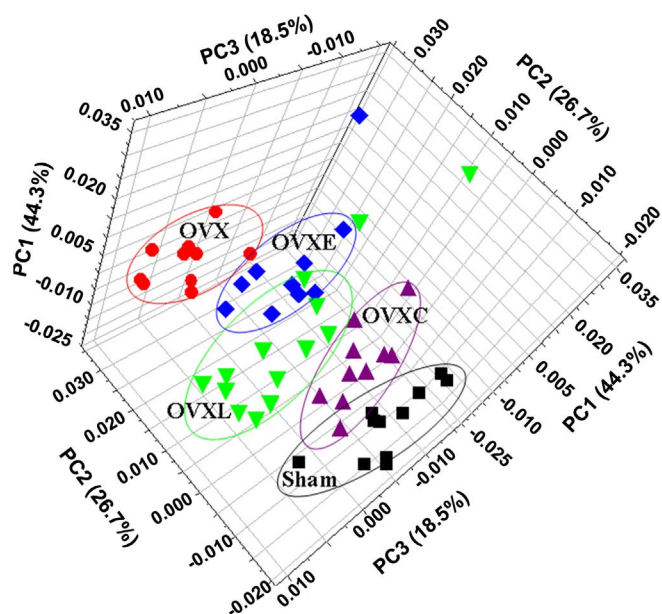
Figure 1 | Three-dimensional PCA scores plot from the plasma metabonomes of sham group (Sham), ovariectomized (OVX) rats, OVX rats treated with nilestriol (OVXE), OVX rats treated with acupoint catgut-embedding (OVXC) and laser-irradiation (OVXL).

β-oxidaton does not. Our observations of the OVX-caused PUFA elevation further indicated that absolute estrogen deficiency promoted the biotransformations from saturated fatty acids to unsaturated fatty acids probably via activation of desaturases. This is consistent with the previous results that stearoyl coenzyme A desaturase-1 (SCD-1) transcription level in OVX rat liver was 41% higher than in sham rat liver[40]. A marked decrease in plasma triglycerides observed here also agreed well with previous findings of reduced hepatic TG secretion in OVX rats[42].

The beneficial effects of acupoint treatments on OVX rats are reflected in the complete restoration for the triglycerides, LDL, HDL, arachidonic acid (AA) and docosahexaenoic acid (DHA) levels in plasma (Table 1). More specifically, catgut-embedding restored all the OVX-induced changes for lipids except for total cholesterol in plasma, whose level was not restored to the normality by any of these treatments (Table 1). In contrast, HRT with nilestriol failed to reverse any of the OVX-induced changes in the lipids except for the levels of LDL (Table 1). This clearly suggested that acupoint stimulations alleviated the OVX-induced perturbations to lipid metabolism to a much greater extent than HRT.

Acupoint stimulations completely reversed the OVX-caused changes of fatty acid oxidative products (i.e., ketone bodies) and restored such to the same levels as for sham rats (Fig. 2) whereas HRT with nilestriol supplementation failed to do so. This further implies that acupoint stimulations can potentially ameliorate oxidative stress induced by the estrogen deficiency (Fig. 3). This is also broadly consistent with the previous findings that acupoint catgut-embedding concurrently can activate superoxide dismutase and reduced malonaldehyde level[43]. Since oxidative stress is one of the most important factors causing cardiovascular diseases, acupoint stimulations are probably superior therapies than HRT for treating postmenopausal woman especially with cardiovascular disease prevention in consideration.

Second, OVX-induced changes in glucose metabolism are also completely reversed by acupoint stimulations. Our results showed that rat blood glucose level in the OVX group was significantly lower than in the sham group (Table 1 and Fig. 2). This appeared to be inconsistent with the known function of estrogen for maintaining

insulin sensitivity[44] and hyperglycemia commonly found in menopausal woman[45]. However, the reported scenario occurred in rats at about sixty-three days after OVX operation[46] and the rise in insulin level was not observed until thirty-five days post-OVX operation[46]. In our analysis, blood plasma was taken ten days after OVX which was well before the rise of insulin level. Our observation of a concurrent increase of plasma citrate level for the OVX rats (Fig. 2) suggested that OVX promoted glycolysis and up-regulation of TCA activity at the early stage of estrogen deficiency (Fig. 3).

Treatments with both acupoint stimulations restored the plasma glucose and citrate levels to what were for the sham rats. HRT also reversed the OVX-induced citrate change. However, HRT failed to restore glucose level to the same level as sham rats and in fact further decreased the blood glucose level. It is nevertheless not known whether such effects of acupoint stimulations on glucose metabolism are long lasting or not. Much longer term acupoint interventions or acupoint interventions at later postmenopausal stages are warranted in the future work.

Third, OVX caused outstanding disruptions in amino acid metabolism which was reflected in the elevations of both essential and non-essential amino acids in blood plasma (Fig. 2). As essential amino acids, branch-chain amino acids (BCAAs) are vital for protein biosynthesis. Disposal and conservation of BCAAs are normally regulated by dephosphorylation and phosphorylation of the branched-chain α-keto acid dehydrogenase complex[47]. Ovariectomy-caused estrogen loss caused the rise of activity for branched-chain α-keto acid dehydrogenase complex[48]. Therefore, the elevation of BCAAs observed here was probably due to the OVX-induced activation of the branched-chain α-keto acid dehydrogenase complex[48].

Menopausal symptoms are also related to disruptions to the nerve and endocrine systems due to dysfunctions of hormones and neurotransmitters. Tyrosine and phenylalanine are precursors for biosynthesis of three important neurotransmitters (i.e., dopamine, epinephrine and norepinephrine) which are related to menopausal symptoms such as depression, fatigue, appetite loss and headaches. Therefore, the elevations of tyrosine and phenylalanine observed here are probably related to the OVX-caused inhibition to biosynthesis of the above neurotransmitters and thus development of menopausal symptoms.

Acupoint interventions alleviated the OVX-induced disruptions in amino acid metabolism to a much greater extent than nilestriol supplementation (Fig. 2). For example, nilestriol supplementation only restored lysine, glycine and arginine levels to normality. In contrast, catgut-embedding also reversed the levels of tyrosine and phenylalanine to normality whilst laser-irradiation restored the levels of BCAAs to the levels for the sham rats (Fig. 2). This suggests that acupoint stimulations are more effective in alleviating the adverse effects of estrogen deficiencies on amino acid metabolisms than nilestriol supplementation. Previous results also suggested that acupuncture acted as a neuromodulating input impinging on the central nervous system, yielding the ultimate therapeutic effects[49]. Therefore, we hypothesized that the effectiveness of acupoint treatments to menopause might result from stimulations to nerve systems accompanied with modulations to protein biosynthesis and amino acids metabolisms.

Ovariectomy-caused significant elevations for AST and ALT (Table 1) indicated that OVX-induced estrogen loss also resulted in liver dysfunctions. HRT with nilestriol failed to alleviate such dysfunctions but further induced ALP decrease being common for postmenopausal women receiving estrogen therapy due to osteoporosis. In contrast, acupoint stimulations with both catgut-embedding and laser-irradiation completely restored the AST and ALT levels to normality (Table 1) indicating their effective therapeutic effects.

Finally, bilateral ovariectomy induced significant increases in acetylglycoproteins (NAG and OAG) in the plasma of OVX rats (Fig. 2).
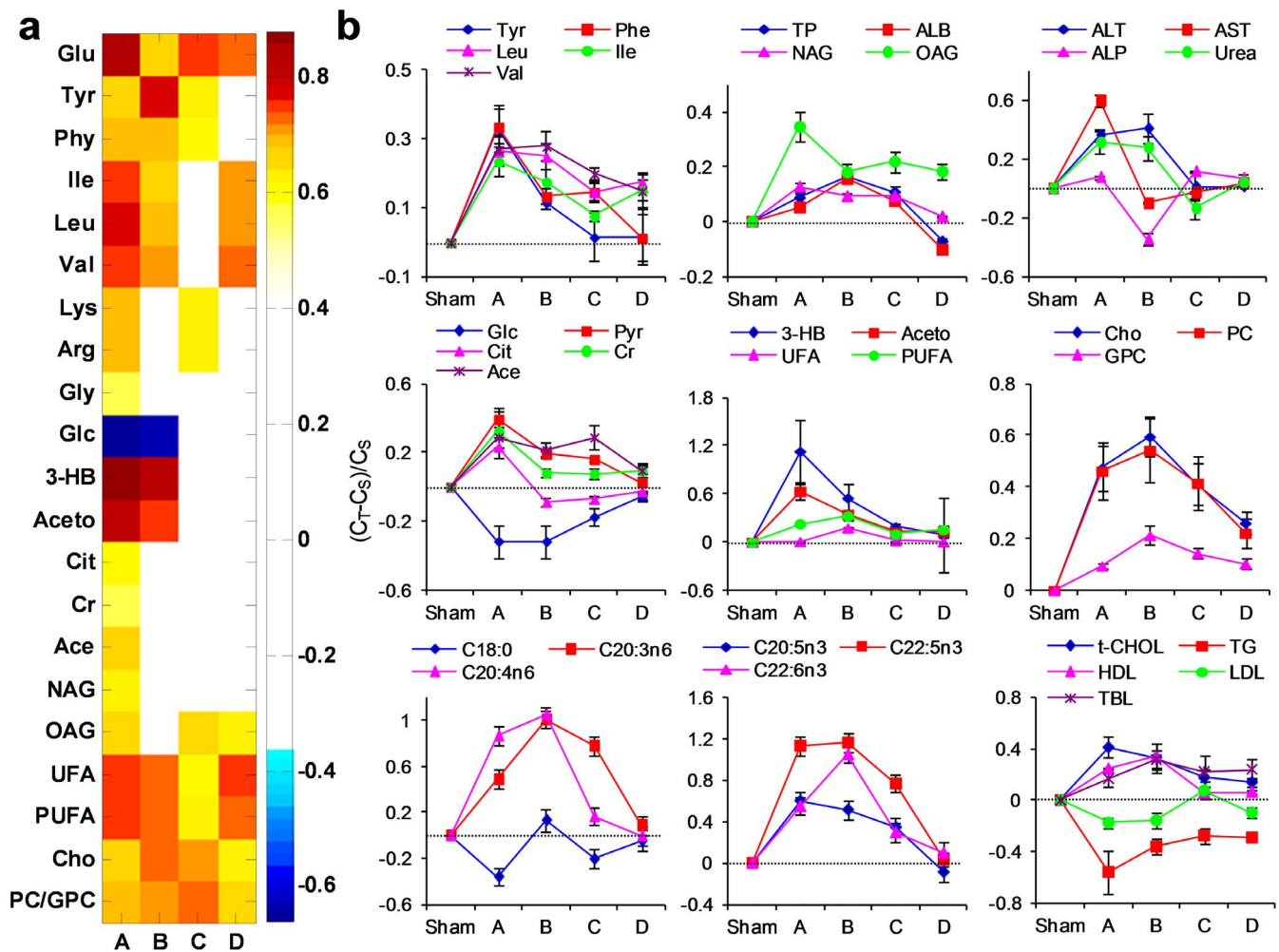
Figure 2 | Alterations of key plasma metabolites of ovariectomized (OVX) rats (A), OVX rats treated with nilestriol (B), OVX rats treated with acupoint laser-irradiation (C) and catgut-embedding (D). (a) Heat-map for metabolite changes color-scaled with correlation coefficients where warm color denotes an increase of metabolite levels whereas cold color (blue) indicates a decrease in the treated rats with respect to the sham group; colorless blocks meant no significant changes against the sham group. (b) The treatment-caused rat metabolite changes against metabolite levels in plasma in the sham group (see experimental section for details) for the ovariectomized rats (A), OVX rats treated with nilestriol (B), OVX rats treated with acupoint laser-irradiation (C) and catgut-embedding (D). C_S and C_T are metabolite levels in the sham and treated groups, respectively. Lines are visual guidance only.

This indicated the OVX-induced promotion of inflammations since NAG and OAG in rat blood plasma were well accepted as "acute-phase" glycoproteins under inflammatory conditions[50]. Concurrent elevations of choline, PC and GPC observed in the OVX rat plasma further support the OVX-induced inflammation since these metabolites are degradation products from of cell membranes (Fig. 3). All three treatments failed to reverse the changes of these choline metabolites. Unlike HRT with nilestriol which reversed the OVX-induced changes of both NAG and OAG, acupoint-stimulations did not completely reverse the OVX-induced changes in OAG. These indicated that all three treatments had only limited effects of alleviating inflammation.

To conclude, these results suggest that acupoint stimulations have profound beneficial effects of rebalancing many of the OVX-induced metabolic alterations. Such was reflected in comprehensive alleviation of the OVX-induced lipid peroxidation, oxidative stress and disruptions in glucose and amino acid metabolisms (Fig. 3). It was particularly interesting to note that acupoint stimulations employed in this study were much more effective than HRT in rebalancing the menopause-caused metabolic alterations. Currently planned work in clinic settings will be valuable to verify these

findings in animal models and translate such findings into treatments for postmenopausal women. Future studies are also required for longer term acupoint interventions and/or acupoint interventions at the later stage of postmenopause. Nevertheless, it is obvious that this work will encourage more metabonomics applications in understanding the biochemical aspects of many effective treatments in translational medicines.

Methods

Animal experiments and sample collection. Animal experiments were performed according to the National Guidelines for Experimental Animal Welfare (the Ministry of Science and Technology, People's Republic of China, 2006) and were approved by the Local Animal Welfare Committee with permission No.0081814. Sixty-five mature female Sprague-Dawley rats (250 ± 20 g, 12-weeks old) were purchased from Experimental Animal Center of Guangzhou University of Chinese Medicine and housed in groups of five at a certified local animal experimental laboratory with a 12 hr light/dark cycle at a constant temperature of 20 ± 2°C. Animals were allowed to have free access to food and water.

After acclimatization for one week, 44 rats were subjected to bilateral ovariectomy (OVX) operation under anesthesia with ethylurethane solution (25% v/v, dosage of 900 mg/kg) whereas 11 rats were subjected to the same operation without removal of ovaries (sham group). The remaining 10 rats were used as control group. The operated rats were allowed to recover for 10 days after surgery. During the period of recovery, all the OVX rats were validated by examining coat of vaginal shelling cells
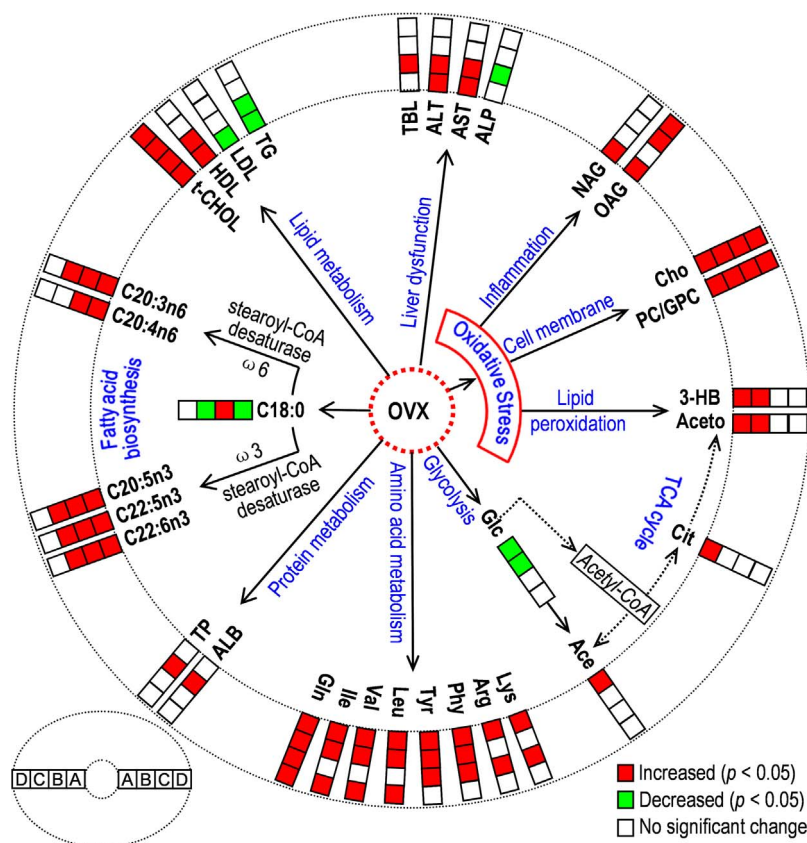
Figure 3 | Summary of metabolic pathways responded to bilateral ovariectomy (A) followed by interventions with nilestriol (B), acupoint laser-irradiation (C) and catgut embedding (D). Abbreviations for all metabolites are listed in the abbreviation list.

(>50%), which is consistent with the characteristics of menopause. After 10 days' recovery, 10 of the OVX rats were gavaged with 0.2 g/L nilestriol solution (5 ml/kg) once every 5 days for 20 days and another 10 OVX rats were treated with catgut-embedding acupoints at bilateral *Shenshu* (BL 23), bilateral *Sanyinjiao* (SP 6) and *Guanyuan* (CV 4) (Fig. S1). Catgut-embedding procedure was performed by introducing catgut lines into the acupoints via a needle with the catgut lines staying in the acupoints as a constant stimulus for about a week before being absorbed. This treatment was performed once every 5 days for 20 days. The third group of OVX rats (n = 14) were subjected to laser-irradiation stimulation to acupoint *Shenshu* (BL 23). The laser-irradiation was conducted with the pulse power of 50 mw, wave length of 808 nm, and beam diameters of 5 mm for 5 minutes daily for 5 days. Such treatment was repeated for 4 times with two days interval.

All animals were then sacrificed by cervical dislocation on the 5th day after the last treatment. Blood samples were collected from the orbital plexus into Eppendorf tubes containing sodium heparin to obtain plasma samples with standard procedures. Samples were then stored at −80°C for later analysis. Partial plasma samples were used for clinical biochemistry examination with standard procedures. Bodyweights and pituitary ERα expression were reported previously[17].

Clinical biochemistry. Clinical biochemistry analysis was carried out with standard methods including alanine aminotransferase (ALT), aspartate aminotransferase (AST), alkaline phosphatase (ALP), albumin (ALB), glucose (Glc), triglycerides (TG), total protein (TP), total cholesterol (t-CHOL), direct bilirubin (DBL), total bilirubin (TBL), urea, high-density lipoprotein (HDL), and low-density lipoprotein (LDL). Obtained data were analyzed using SPSS 13.0 software with a Turkey post-test (one way-ANOVA) for inter-group discrimination significances.

^{1}H NMR spectroscopy of rat plasma. Plasma samples were prepared by mixing 200 μL of plasma with 400 μL of saline solution containing 50% D_2O (as a field lock) and 550 μL of samples was transferred into 5 mm NMR tubes after vortex and 10 min centrifugation (4°C, 11180 *g*).

All ^{1}H NMR spectra of plasma were recorded at 298 K on a Bruker Avance III 600 MHz spectrometer (Bruker Biospin, Germany) equipped with a cryogenic inverse detection probe. Three NMR spectra were recorded for each sample, namely, NOESYPR1D spectrum, Carr-Purcell-Meiboom-Gill (CPMG) NMR spectrum and diffusion-edited NMR spectrum. 90° pulse was adjusted to 10 μs for each sample and water signal was suppressed with a weak continuous wave irradiation. 32 K data points were collected for each spectrum with a spectral width of 20 ppm and recycle delay of 2 s. Mixing time was 100 ms for NOESYPR1D spectra whereas the total spin-spin relaxation delay, 2nτ, was set to 96 ms for CPMG spectra. Diffusion-edited

spectra were acquired as previously reported[51] with diffusion time of 200 ms and pulse-field gradient strength of 31.2 G/cm (Fig. S6). All free induction decays were multiplied by an exponential function with a 1 Hz line broadening factor prior to Fourier transformation (FT). All spectra were referenced to the anomeric proton signal of α-glucose (δ5.233).

For the purposes of NMR signal assignments, a series of 2D NMR spectra were acquired and processed for selected samples as described previously[36,52,53] including[1]H-^{1}H correlation spectroscopy (COSY),[1]H-^{1}H total correlation spectroscopy (TOCSY),[1]H J-Resolved,[1]H-^{13}C heteronuclear single quantum correlation (HSQC) and heteronuclear multiple bond correlation spectra (HMBC).

GC-FID/MS analysis of fatty acid composition (or fatty acid metabonome). Plasma fatty acids were methylated with acetyl chloride as catalyst as reported previously[54,55] with some modifications. In brief, 20 μl internal standards (methyl esters of C17:0 and C23:0) in hexane containing butylated hydroxytoluene (BHT) was added to a 12 ml Pyrex tube followed with addition of 100 μl rat plasma and 4 ml methanol-hexane mixture (4 : l, v/v). The sample tubes were placed above a liquid N_2 bath for 10 min to cool down. 200 μl pre-cooled acetyl chloride was added to the above mixture followed with a brief nitrogen gas flush. Tubes were then screw-capped and kept at room temperature in the dark for 24 h. The resultant mixture was cooled in an ice bath for 10 min and then added with 5 ml of 6% K_2CO_3 solution slowly (with shaking) to neutralize. After standing for 30 min, the mixture was added with 200 μl of hexane. Following another 10 min resting, the top layer was collected and transferred to a sample vial. Above extraction process was repeated three times and the combined supernatants were evaporated to dryness. The resultant residues were then redissolved in 50 μl hexane for GC-FID/MS analysis.

Fatty acid composition was measured on a Shimadzu GCMS-QP2010Plus spectrometer (Shimadzu Scientific Instruments, USA) equipped with a flame ionization detector (FID). A DB-225 capillary GC column (10 m, 0.1 mm ID, 0.1 μm film thickness) was employed with helium as carrier and make-up gas. Sample injection volume was 1 μl with a splitter (1 : 60). The injection port and detector temperatures were both set to 230 °C. The column temperature was set to 55°C for 0.5 min and then increased to 205°C with a rate of 30°C/min. Colum temperature was kept at 205°C for 3 min then increased to 230°C (5°C/min) and kept at 230°C for 2.5 min. Fatty acids were quantified by FID data by comparing with signal integrals of internal standards.

NMR Data processing and multivariate data analysis. After manual phase- and baseline-corrections, each[1]H NMR spectrum (δ 0.5–9.5) was segmented into bins with equal width of 0.004 ppm (2.4 Hz) using AMIX software package (V3.8, Bruker

Biospin, Germany). The regions containing water (δ 4.4–5.1) and urea (δ 5.5–6.0) signals were discarded prior to further analysis.

Multivariate data analysis was conducted with SIMCA-P$^+$ package (V12.0, Umetrics, Sweden). Principal component analysis (PCA) was performed on the mean-centered data to generate an overview and identify outliners. Partial least-squares-discriminant analysis (PLS-DA) and orthogonal projection to the latent structure with discriminant analysis (OPLS-DA) were subsequently conducted using the unit-variance scaled NMR data as X-matrix and class information as Y-matrix. The quality of OPLS-DA models were ensured with a seven-fold cross-validation method and further assessed with the CV-ANOVA method[56]. After back-transformation[57], the loadings from the OPLS-DA models were plotted using an in-house developed Matlab script (V7.1, The Mathworks, MA) with correlation coefficients color-coded to reflect the significance of inter-group differentiations for all metabolites. The hot colored (e.g., red) variables (or metabolites) are more significantly contributed to inter-group differences than cool ones (e.g., blue). A cutoff value of 0.602 for the correlation coefficient (i.e., $|r| > 0.602$) was chosen to select metabolites with statistical significance between groups ($p < 0.05$) according to the discriminating significance of the Pearson's product-moment correlation coefficient[57]. The Student's t-tests were also done for clinical biochemistry and plasma fatty-acids data (Table 1).

The treatment-caused metabolite changes were calculated against their plasma concentration from sham rats, i.e., $(C_T-C_S)/C_S$, where C_T and C_S were concentration of a given metabolite in plasma of treated and sham rats, respectively. Since concentration of a given metabolite is linearly proportional to its signal integral in NMR spectra, integrals of the least overlapping signals from concerned metabolites have been employed in the above calculation.

1. Blake, J. Menopause: evidence-based practice. *Best. Pract. Res. Clin. Obstet. Gynaecol.* **20**, 799–839 (2006).
2. Sormova, I. & Donat, J. Risk factors of metabolic estrogen-deficiency syndrome in women after menopause and its relationship to hormone replacement therapy. *Ceska. Gynekol.* **69**, 388–396 (2004).
3. Oztekin, E., Tiftik, A. M., Baltaci, A. K. & Mogulkoc, R. Lipid peroxidation in liver tissue of ovariectomized and pinealectomized rats: effect of estradiol and progesterone supplementation. *Cell Biochem. Funct.* **25**, 401–405 (2007).
4. Utian, W. H. Quality of life (QOL) in menopause. *Maturitas* **57**, 100–102 (2007).
5. Cabero, A. Hot flashes, menopause, nitric oxide and hormone replacement therapy: "one for all and all for one" *Med. Clin.* **114**, 52–53 (2000).
6. Riis, B. J., Hansen, M. A., Jensen, A. M., Overgaard, K. & Christiansen, C. Low bone mass and fast rate of bone loss at menopause: equal risk factors for future fracture: a 15-year follow-up study. *Bone* **19**, 9–12 (1996).
7. Philosophe, R. & Seibel, M. M. Menopause and cardiovascular disease. *NAACOGS Clin. Issu. Perinat. Womens Health Nurs.* **2**, 441–451 (1991).
8. Mooren, V. M. & Kenemans, P. Postmenopausal hormone therapy: impact on menopause- related symptoms, chronic disease and quality of life. *Drugs* **64**, 821–836 (2004).
9. Ushioda, M., Makita, K., Takamatsu, K., Horiguchi, F. & Aoki, D. Serum lipoprotein(a) dynamics before/after menopause and long-term effects of hormone replacement therapy on lipoprotein(a) levels in middle-aged and older Japanese women. *Horm. Metab. Res.* **38**, 581–586 (2006).
10. Hwang, J. et al. Long-term effect of estrogen replacement on plasma nitric oxide levels: results from the estrogen in the prevention of atherosclerosis trial (EPAT). *Atherosclerosis* **181**, 375–380 (2005).
11. Taskin, O., Trak, B., Mendilcioglu, I. & Saka, O. Clarifications and relationships between estrogen and prostaglandins. *Fertil. Steril.* **73**, 873–874 (2000).
12. LaCroix, A. Z. & Burke, W. Breast cancer and hormone replacement therapy. *Lancet* **11**, 1042–1043 (1997).
13. Mørch, L. S., Løkkegaard, E., Andreasen, A. H., Krüger-Kjaer, S. & Lidegaard, O. Hormone therapy and ovarian cancer. *JAMA* **15**, 298–305 (2009).
14. Turner, J. V., Agatonovic-Kustrin, S. & Glass, B. D. Molecular aspects of phytoestrogen selective binding at estrogen receptors. *J. Pharm. Sci.* **96**, 1879–1885 (2007).
15. Wyon, Y., Wijma, K., Nedstrand, E. & Hammar, M. A comparison of acupuncture and oral estradiol treatment of vasomotor symptoms in postmenopausal women. *Climacteric.* **7**, 153–164 (2004).
16. Zaborowska, E. et al. Effects of acupuncture, applied relaxation, estrogens and placebo on hot flushes in postmenopausal women: an analysis of two prospective, parallel, randomized studies. *Climacteric.* **10**, 38–45 (2007).
17. Zhang, Y. et al. Effects of laser irradiation of acupuncture points Shenshu on ovariectomized rats. *Photomed Laser Surg.* **29**, 271–275 (2011).
18. Shi, Y., Zhang, L. S., Zhao, C. & He, C. Q. Comparison of therapeutic effects of acupuncture-cupping plus acupoint catgut embedding and electroacupuncture on simple obesity of stomach and intestine excess-heat type. *Zhongguo Zhen Jiu* **26**, 547–550 (2006).
19. Ouyang, H. & Chen, J. D. Review article: therapeutic roles of acupuncture in functional gastrointestinal disorders. *Aliment Pharmacol. Ther.* **20**, 831–41 (2004).
20. Zhang, H., Bian, Z. & Lin, Z. Are acupoints specific for diseases? A systematic review of the randomized controlled trials with sham acupuncture controls. *Chin. Med.* **5**, 1 (2010).
21. Acupuncture. NIH Consensus Statement 1997 Nov 3–5; 15(5):1–34. http://consensus.nih.gov/1997/1997acupuncture107html.htm. (Accessed on September 29 2013).
22. Acupuncture - Evidence. http://www.nhs.uk/conditions/acupuncture/pages/evidence.aspx (Accessed on September 29 2013).
23. Zhang, X. R. Acupuncture: review and analysis of reports on controlled clinical trials. http://apps.who.int/medicinedocs/pdf/s4926e/s4926e.pdf. (Accessed on November 21 2013).
24. Menopausal Symptoms and Complementary Health Practices. http://nccam.nih.gov/health/acupuncture (Accessed on September 29 2013).
25. Nicholson, J. K., Lindon, J. C. & Holmes, E. 'Metabonomics': understanding the metabolic responses of living systems to pathophysiological stimuli via multivariate statistical analysis of biological NMR spectroscopic data. *Xenobiotica* **29**, 1181–1189 (1999).
26. Tang, H. R & Wang, Y. L. Metabonomics-a revolution in progress. *Prog. Biochem. Biophys.* **33**, 401–417 (2006).
27. Wang, Y. L. et al. Global metabolic responses of mice to *Trypanosoma brucei brucei* infection. *Proc. Natl. Acad. Sci. U S A* **105**, 6127–6132 (2008).
28. Wu, J. F. et al. Metabolic changes reveal the development of schistosomiasis in mice. *PLoS Negl. Trop. Dis.* **4**, e807–e818 (2010).
29. Yang, Y. X. et al. Metabonomic studies of human hepatocellular carcinoma using high-resolution magic-angle spinning ^{1}H NMR spectroscopy in conjunction with multivariate data analysis. *J. Proteome Res.* **6**, 2605–2614 (2007).
30. Li, H. et al. Transcriptomic and metabonomic profiling of obesity-prone and obesity-resistant rats under high fat diet. *J. Proteome Res.* **7**, 4775–4783 (2008).
31. He, Q. H. et al. Comparison of serum metabolite compositions between obese and lean growing pigs using an NMR-based metabonomic approach. *J. Nutr. Biochem.* **23**, 133–139 (2012).
32. Bao, Y. et al. Metabonomic variations in the drug-treated type 2 diabetes mellitus patients and healthy volunteers. *J. Proteome Res.* **8**, 1623–30 (2009).
33. Zhang, X. Y. et al. Human serum metabonomic analysis reveals progression axes for glucose intolerance and insulin resistance statuses. *J. Proteome Res.* **8**, 5188–5195 (2009).
34. Marchesi, J. R. et al. Rapid and noninvasive metabonomic characterization of inflammatory bowel disease. *J. Proteome Res.* **6**, 546–551 (2007).
35. Bjerrum, J. T. et al. Metabonomics in ulcerative colitis: diagnostics, biomarker identification, and insight into the pathophysiology. *J. Proteome Res.* **9**, 954–962 (2010).
36. Ding, L. N. et al. Systems biological responses to chronic perfluorododecanoic acid exposure by integrated metabonomic and transcriptomic studies. *J. Proteome Res.* **8**, 2882–9281 (2009).
37. Tang, H. R., Wang, Y. L., Nicholson, J. K. & Lindon, J. C. Use of relaxation-edited one-dimensional and two dimensional nuclear magnetic resonance spectroscopy to improve detection of small metabolites in blood plasma. *Anal. Biochem.* **325**, 260–272 (2004).
38. Xu, W. X. et al. Streptozotocin-induced dynamic metabonomic changes in rat biofluids. *J. Proteome Res.* **11**, 3423–3435 (2012).
39. Borud, E. & White, A. A review of acupuncture for menopausal problems. *Maturitas* **66**, 131–134 (2010).
40. Paquette, A., Wang, D., Jankowski, M., Gutkowska, J. & Lavoie, J. M. Effects of ovariectomy on PPARα, SREBP-1c, and SCD-1 gene expression in the rat liver. *Menopause* **15**, 1169–1175 (2008).
41. Campbell, S. E. & Febbraio, M. A. Effect of ovarian hormones on mitochondrial enzyme activity in the fat oxidation pathway of skeletal muscle. *Am. J. Physiol. Endocrinol. Metab.* **281**, e803–e808 (2001).
42. Joles, J. A., Bijleveld, C., Tol, A., Geelen, M. J. & Koomans, H. A. Ovariectomy decreases plasma triglyceride levels in analbuminaemic rats by lowering hepatic triglyceride secretion. *Atherosclerosis* **117**, 51–59 (1995).
43. Chen, G. Z., Xu, Y. X., Zhang, J. W., Liu, S. H. & Guo, Z. Y. Effect of acupoint catgut-embedding on the quality of life, reproductive endocrine and bone metabolism of postmenopausal women. *Chin. J. Integr. Med.* **16**, 498–503 (2010).
44. Lee, C. C., Kasa-Vubu, J. Z. & Supiano, M. A. Differential effects of raloxifene and estrogen on insulin sensitivity in postmenopausal women. *J. Am. Geriatr. Soc.* **51**, 683–688 (2003).
45. Chakrabarti, S. & Davidge, S. T. High glucose-induced oxidative stress alters estrogen effects on ERalpha and ERbeta in human endothelial cells: reversal by AMPK activator. *J. Steroid Biochem. Mol. Biol.* **117**, 99–106 (2009).
46. Liu, M. L., Xu, X., Rang, W. Q., Li, Y. J. & Song, H. P. Influence of ovariectomy and 17β-estradiol treatment on insulin sensitivity, lipid metabolism and post-ischemic cardiac function. *Int. J. Cardiol.* **97**, 485–493 (2004).
47. Harris, R. A., Joshi, M. & Jeoung, N. H. Mechanisms responsible for regulation of branched-chain amino acid catabolism. *Biochem. Biophys. Res. Commun.* **313**, 391–396 (2004).
48. Obayashi, M. et al. Estrogen controls branched-chain amino acid catabolism in female rats. *J. Nutr.* **134**, 2628–2633 (2004).
49. Han, J. S. & Terenius, L. Neurochemical basis of acupuncture analgesia. *Annu. Rev. Pharmacol. Toxicol.* **22**, 193–220 (1982).
50. Grootveld, M. et al. High resolution proton NMR investigations of rat blood plasma. Assignment of resonances for the molecularly mobile carbohydrate side-chains of 'acute-phase' glycoproteins. *FEBS Lett.* **322**, 266–276 (1993).

51. Zhang, L. *et al*. Systems responses of rats to aflatoxin B1 exposure revealed with metabonomic changes in multiple biological matrices. *J. Proteome Res.* **10**, 614–623 (2011).

52. Dai, H., Xiao, C., Liu, H. & Tang, H. R. Combined NMR and LC-MS analysis reveals the metabonomic changes in *Salvia miltiorrhiza* Bunge induced by water depletion. *J. Proteome. Res.* **9**, 1460–1475 (2010).

53. Dai, H., Xiao, C., Liu, H., Hao, F. & Tang, H. R. Combined NMR and LC-DAD-MS analysis reveals comprehensive metabonomic variations for three phenotypic cultivars of *Salvia Miltiorrhiza* Bunge. *J. Proteome. Res.* **9**, 1565–1578 (2010).

54. An, Y. P. *et al*. High-fat diet induces dynamic metabolic alterations in multiple biological matrices of rats. *J. Proteome Res.* **12**, 3755–3768 (2013).

55. Li, H. H. *et al*. Combined NMR and GC-MS analyses revealed dynamic metabolic changes associated with the carrageenan-induced rat pleurisy. *J. Proteome Res.* **12**, 5520–5534 (2013).

56. Eriksson, L., Trygg, J. & Wold, S. CV-ANOVA for significance testing of PLS and OPLS (R) models. *J. Chemometrics* **22**, 594–600 (2008).

57. Cloarec, O. *et al*. Evaluation of the orthogonal projection on latent structure model limitations caused by chemical shift variability and improved visualization of biomarker changes in ¹H NMR spectroscopic metabonomic studies. *Anal. Chem.* **77**, 517–526 (2005).

Ackowledgments

Author contributions

L.M.Z. acquired NMR and GC-FID/MS data, conducted data analysis and contributed to manuscript writing, Y.L.W. contributed to data analysis, interpretations and manuscript preparation. H.H.Lei and H.H.Li developed an optimized GC-FID/MS method. Y.Z. contributed to preparation of Figs. 2–3 and Fig. S1. G.Z.C. contributed to the design of the study and conducted animal experiments. Y.X.X. contributed to experimental design, execution and manuscript preparation. X.S.L. performed animal experiments. H.R.T. contributed to the design of the study and supervised the project including data analysis, interpretations and contributed to manuscript preparation.

Additional information